Science and Technology Indonesia
e-ISSN:2580-4391 *p*-ISSN:2580-4405
Vol. 10, No. 1, January 2025

Research Paper

Synthesis of Au-Pd-NPs Materials and Application as Electrochemical Sensor of Hydroquinone in Cosmetics

Riyanto[1*], Safira Mardliyaliari[1], Alya Sabrina[1], Muhammad Ridho[2]

[1]*Department of Chemistry, Chemistry Study Program, Islamic University of Indonesia, Sleman, 55584, Indonesia*
[2]*Department of Chemistry, Magister Chemistry Study Program, Islamic University of Indonesia, Sleman, 55584, Indonesia*
***Corresponding author**: riyanto@uii.ac.id

Abstract
Hydroquinone is a hazardous and toxic chemical often added to cosmetics due to bleaching properties. It is commonly analyzed in cosmetics using expensive and time-consuming instruments, showing the need for a cheap, fast, and sensitive hydroquinone electrochemical sensor. The performance of electrochemical sensor to detect hydroquinone is determined by the working electrode. Therefore, this study aimed to explore the synthesis of Au-Pd-NPs working electrode and application as electrochemical sensor of hydroquinone in cosmetics. Synthesis process was carried out by preparing Au-NPs using banana peel extract (*Musa acuminata* Colla) as a bioreductor, followed by adding H_2PdCl_4 solution. Au-NPs nanoparticle was confirmed using Ultraviolet-Visible spectrophotometer, which showed maximum wavelength of 550 nm. The indication of Au-Pd-NPs was shown by the peak at the same wavelength. The FTIR spectrum showed pectin which acted as a bioreductant agent in synthesis of nanoparticles. The results of the TEM image showed that Au-NPs had a spherical shape in the dark field with a diameter of 38.5 ± 3.3 nm and a Pd shell layer around the Au core in the bright field with a diameter of 12.4 ± 2.6 nm. The solid Au-Pd-NPs materials were made into a composite electrode by adding PVC and tetrahydrofuran as solvents. Electrochemical response of Au-Pd-NPs electrode was tested by cyclic voltammetry in ferricyanide and PBS solutions at pH 7.0. Based on CV in the ferricyanide system, it shows that Au-Pd-NPs electrode produces peak oxidation and reduction currents ten times higher than Au-NPs. These data indicate that Au-Pd-NPs are more reactive and sensitive than Au-NPs electrodes. The Au-Pd-NPs electrode was used to analysis the concentration of hydroquinone in cosmetics samples. Electrochemical response showed a linearity (R^2) of 0.9935 in concentration range of 0-60 mM, containing 1.12% hydroquinone.

Keywords
Au-Pd-NPs, Sensor, Hydroquinone, Cosmetics Synthesis

Received: 12 September 2024, Accepted: 18 December 2024
https://doi.org/10.26554/sti.2025.10.1.294-302

1. INTRODUCTION

A total of 39 types of cosmetics were identified in 2016 by the Food and Drug Supervisory Agency (BPOM). These included 25 local and 14 imported product brands containing hazardous chemicals, dominated by decorative cosmetics and skin care products. Many of these products contain 46.16% red dye rhodamine B as well as 17.95% hydroquinone and mercury (Nurhan et al., 2017). However, the use of hydroquinone has been prohibited as a bleach in cosmetics in the Regulation of the Head of BPOM in 2011 concerning Technical Requirements for Cosmetic Ingredients (Chakti et al., 2019). Hydroquinone is widely used as a skin bleach by inhibiting the formation of melanin through the enzyme tyrosinase and skin depigmentation. Although hydroquinone is capable of treating hyperpigmented skin, long-term use can have harmful effects such as inflammation or irritation of the skin, damage to melanin-producing cells, ochronotic, post-inflammatory, and nail discoloration (Adebajo, 2002). Based on the European Commission, the use of hydroquinone has been banned in cosmetics (Siddique et al., 2012; Elferjani et al., 2017). According to Cosmetic Safety Regulation of the EU, a significant proportion is permitted at concentrations of approximately 2% (Lin et al., 2005).

Several studies have shown that hydroquinone is carcinogenic and mutagenic, with a high level of toxicity. It is low in decomposition, causing harmful effects on humans, animals, and the environment. Hydroquinone toxicity can cause severe side effects such as kidney and liver damage, cancer, blood poisoning, nausea, stomach pain, seizures, and coma (Wang et al., 2017; Elferjani et al., 2017). Dermatologists have shown that long-term use of products containing this chemical causes accumulation in the body capable of damaging the outer

protective layer of the skin and temporary or permanent skin discoloration. This phenomenon damages nerves, leading to kidney failure or skin cancer (Westerhof and Kooyers, 2005). Hydroquinone can cause neurological effects including dizziness and headaches, ringing in the ears, severe confusion or dazedness that makes it difficult for sufferers to focus and think, and green to greenish brown urine (Melisa and Jay, 2009).

Several research have been conducted to obtain the best method for the determination of hydroquinone content. These include (HPLC) high-performance liquid chromatography (Desiderio et al., 2000; Pistonesi et al., 2006; Sotomayor et al., 2022), spectrometry (Lei et al., 2007; Aziz et al., 2007), chemiluminescence (Tsai and Chiu, 2007; Mersal, 2009), capillary electrochromatography (Zhao et al., 2009), and fluorescence (Khoshroo et al., 2018). Despite the significant contribution, these methods have many disadvantages such as high operational costs, complicated sample pretreatment, long analysis time, limited sensitivity, high detection limits, and require special expertise, thereby limiting their application.

In this context, electrochemical sensor method is an alternative method for the efficient determination of hydroquinone levels due to high sensitivity, rapid detection, cost-effectiveness, and good selectivity (Li et al., 2018; Liu et al., 2018; Du et al., 2019; Pereira et al., 2020; Bhardwaj et al., 2017; Shore et al., 2016). The selective and sensitivity of electrochemical sensors is significantly affected by the conductivity and surface area of the material used. The performance can be improved by modifying the electrode with including metal, metal oxides, various nanomaterials, and carbon materials. Additionally, gold-palladium (Au-Pd) nanoparticles are bimetallic nanomaterials that have been widely used in the biosensor field because it has high catalytic properties and a large surface area (Kumar and Goyal, 2017). Metal-based nanoparticles have been widely applied in sensor applications because they have unique optical properties and sensitive and selective physicochemical properties. Metal nanoparticles in enhancing the response in electrochemical sensors through electrocatalytic effects and electron transfer facilities. Metal nanoparticles can be synthesized with the desired size and shape (Khan et al., 2019). Metal nanoparticles that can be used in electrochemical sensors are gold-palladium with a core-shell structure (Au-Pd-NPs).

In this research, the synthesis of Au-Pd-NPs was carried out using Au-NPs. Au-NPs were synthesized using banana (*Musa acuminata* Colla) peel extract as a bioreductor. Banana peel is a biomass containing starch, lignin, cellulose, hemicellulose, and pectin which is an important function in chemical synthesis (Thongnopkun et al., 2018). In addition, banana peels contain antioxidants such as polyphenols which are higher than fruit, so it has the potential to be used as a reductant in nanoparticle synthesis. Banana peel waste has the potential to be used in nanoparticle synthesis (Chafidz et al., 2020).

2. EXPERIMENTAL SECTION

2.1 Materials and Instrumentation

The materials used included gold bullion (99.999%, Antam), 37% concentrated hydrochloric acid (HCl), 65% concentrated nitric acid (HNO_3), 97% concentrated sulfuric acid (H_2SO_4), palladium (II) chloride ($PdCl_2$), phosphate-buffered saline (PBS), tetrahydrofuran (THF), and potassium ferricyanide ($K_3[Fe(CN)_6]$). Other materials were potassium ferrocyanide ($K_4[Fe(CN)_6]$), polyvinyl chloride ($(C_2H_3Cl)_n$), hydroquinone ($C_6H_6O_2$), copper wire (Cu), silver conductive paint, banana peel, cosmetics products, and demineralized water. The instrumentation used in this study was Cyclic Voltammetry (CV) brand μAutolab Type III, UV-Visible Double Beam Spectrophotometer brand Hitachi U-2900, Fourier Transform InfraRed (FTIR) brand Nicolet Avatar 360 IR, and Transmission Electron Microscopy (TEM) brand Jeol JEM-1400.

2.2 The Extraction of Banana (*Musa acuminata* Colla) Peel

Banana (*Musa acuminata* Colla) peel extract was made by cleaning the banana peel and cutting into small pieces, weighing 30 g, and putting it into a beaker. The material was then dissolved in 100 mL of demineralized water and then heated for 30 minutes at 80 °C. The mixture obtained was filtered and the banana peel extract solution as a reducing and stabilizing agent was made with a concentration of 5% (v/v).

2.3 Preparation of Chloroauric Acid $HAuCl_4$, and H_2PdCl_4 Solution

$HAuCl_4$ 50 mM solution was made from 0.5 g of gold metal put into a beaker, followed by adding 40 mL of HCl 37%, and 10 mL of HNO_3 65%. The mixture was stirred in a fume hood and heated to allow for acid evaporation. Subsequently, the solution obtained was added with demineralized water to a volume of 50 mL. Another $HAuCl_4$ 50 mM solution was made by taking 2.5 mL of 50 mM $HAuCl_4$ stock solution and putting in a 25 mL measuring flask, which was added with 0.2 M H_2SO_4 solution. Amount 44.5 mg of $PdCl_2$ solids were dissolved in 20 mM HCl, heated, and stirred to obtain a 10 mM H2PdCl4 solution (Liu et al., 2015).

2.4 Synthesis of Au-Pd-NPs

Au-NPs synthesis was carried out by taking 1 mL of 5 mM $HAuCl_4$ and adding 100 mL of 5% banana peel extract. The mixture was stirred for 1 hour until a red-purple color was produced. Meanwhile, Au-Pd-NPs synthesis was carried out by adding Au-NPs solution to 10 mM H_2PdCl_4 (4:1 (v/v)) and then stirring at 35 °C for 2 hours until a brown solution was produced, showing successful synthesis. The Au-Pd-NPs solution was heated until dry and the powder was formed.

2.5 Preparation of Au-Pd-NPs Working Electrode

Au-Pd-NPs working electrode was prepared by adding 2.5 mg of PVC powder to 47.5 mg of Au-Pd-NPs powder (ratio 5:95 (% w/w)), stirred until homogeneous. The mixture was added

with 3 drops of THF solution, dried, pressed using a 1 cm diameter mold and heated at 50 °C for 1 hour. Silver conductive paint was applied to electrode surface, connected with copper (Cu) wire, and dried for 24 hours at room temperature. The Cu wire was inserted into a glass pipe and the part in contact with the solution was covered with epoxy. The working electrode was left for 24 hours at room temperature before use, followed by characterization of banana peel extract, Au-NPs, and Au-Pd-NPs using UV-visible spectrophotometer, FTIR, and TEM. Synthesis steps of HAuCl4, Au-NPs, Au-Pd-NPs, and preparation as working electrode of Au-Pd-NPs are shown in Figure 1.

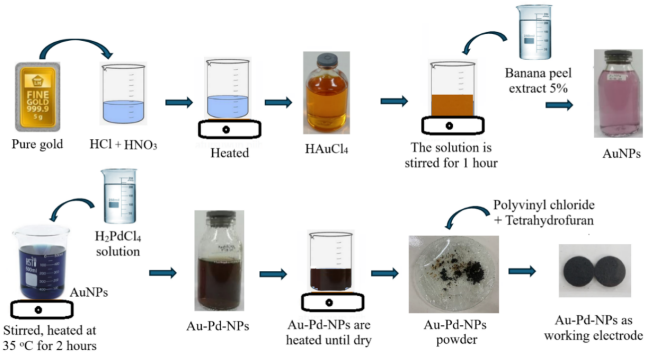

Figure 1. Synthesis Steps of $HAuCl_4$, Au-NPs, Au-Pd-NPs and Preparation as Working Electrode Au-Pd-NPs

2.6 Electrochemical Response of Au-Pd-NPs Electrode

The activity of Au-Pd-NPs electrode was analysis using cyclic voltammetry (CV) in ferricyanide solution. The solution used was $K_3[Fe(CN)_6]/K_4[Fe(CN)_6]$ 10 mM solution (1:1 molar ratio) with 1 M KCl electrolyte. The potential measurement was carried out at -0.65 to 0.5 V with a scan rate of 0.01-0.03 V/s. Subsequently, 1.1 g of hydroquinone was weighed, dissolved in demineralized water, and put into a 100 mL volumetric flask to obtain a 100 mM hydroquinone stock solution. Hydroquinone working solutions with concentrations of 0, 10, 20, 30, 40, 50, and 60 mM. A total of 25 mL hydroquinone was added with 5 mL of PBS solution (pH 7.0) analyzed by cyclic voltammetry. Hydroquinone analysis was carried out by dissolving 1 g of cosmetics sample in 20 mL of demineralized water, stirring for 10 minutes, filtering, and analyzing by cyclic voltammetry. Measurement of hydroquinone concentration in cosmetics samples was performed in duplicate (two repetitions) with a potential of -0.5 to 1 V and a scan rate of 0.015 V/s.

3. RESULT AND DISCUSSION

3.1 Characterization of Banana Peel Extract, Au-NPs, and Au-Pd-NPs

Figure 2 shows the difference in solution color between $HAuCl_4$, Au-NPs, and Au-Pd-NPs. The formation of Au-NPs was evidenced by the solution color from yellow to purple. After the analysis of Au-NPs, the formation of Pd layer was continued by adding H_2PdCl_4 solution. Banana peel extract contained flavonoids as reducing agents and stabilizing agents, which reduced Au^{3+} to Au^o. This led to the formation of Au-NPs core, which was added with the precursor $PdCl_4^{2-}$. The excess reducing agent of banana peel extract reduced $PdCl_4^{2-}$ to Pdo to form the Pd shell, with brown solution showing Au-Pd-NPs, as presented in Figure 2c.

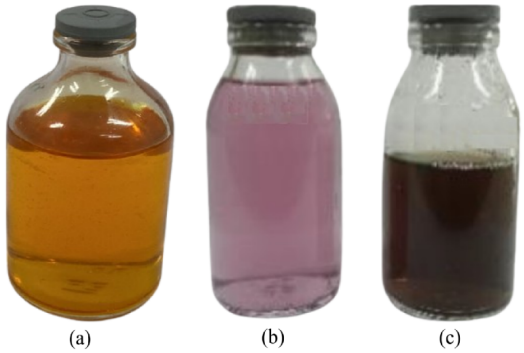

Figure 2. Visual $HAuCl_4$ (a), Au-NPs (b), and Au-Pd-NPs (c)

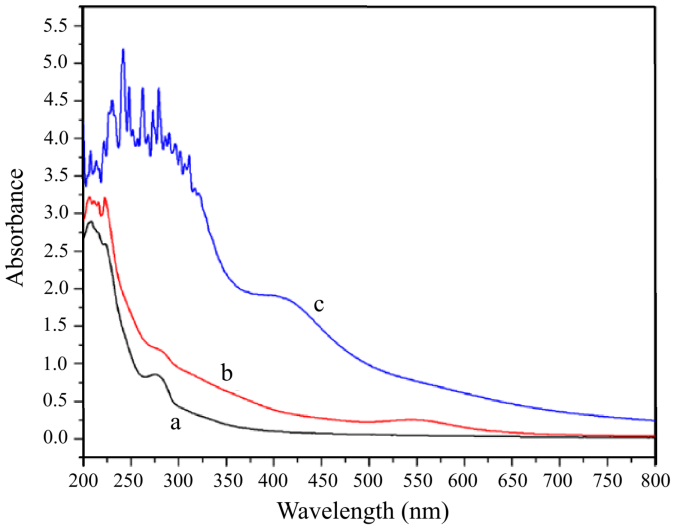

Figure 3. UV-Visible Spectrum of 5% Banana Peel Extract (a), Au-NPs (b), and Au-Pd-NPs (c)

Figure 3 shows the spectra of banana peel extract, Au-NPs, and Au-Pd-NPs from synthesis process. Generally, most metal nanoparticles produce surface plasmon resonance (SPR) absorption bands because they have free electrons. This is because the vibrations of electrons resonate with electromagnetic waves in the form of light waves. Gold has an atomic number of 79, showing 79 electrons, with an electron configuration of [Xe] $4f^{14}5d^{10}6s$. The outermost electron shell contains one electron from the s orbital. Meanwhile, palladium has an atomic number of 46, and contains 10 electrons in the d orbital, with

an electron configuration of [Kr] $4d^{10}$. The electron configuration of gold and palladium affects the electronic properties of nanoparticles, including the density of free electrons available for SPR. Plasmonic nanoparticles (noble metals) are known to show unique optical properties due to their SPR properties (Bindhu and Umadevi, 2013). These optical properties result from the participation of free electron particles in the collective oscillation of electrons. Free electrons undergo collective oscillations at the interface between the metal and the dielectric material to produce SPR. When light interacts with a metal surface, it drives s-electrons and d-electrons to higher energy levels or electron excitation, thereby creating collective oscillations. The frequency of incident light matches the natural frequency of collective electron oscillations, which can cause resonance. This resonance causes increased absorption or scattering of light, leading to characteristic dips or peaks in the absorption spectrum. The intensity of the SPR band and wavelength are influenced by several factors such as the density of electron charge on the particle surface. According to Mie Theory, the electron charge density is influenced by the type of metal, shape, particle size, dielectric constant of the surrounding medium, composition, and structure (Huang and El-Sayed, 2010).

In this study, initial detection was carried out to determine whether nanoparticles were formed through visual observation of solution color change. This change was caused by SPR excitation on the surface of metal nanoparticles. When synthesizing the Au-NPs core, there was a color change from pale yellow to purplish, which showed the formation of Au-NPs. Synthesis of Au-Pd-NPs continued through the formation of Pd shell, where there was a color change from purple to brown. This was followed by the analysis of Au-Pd-NPs using a UV-Visible spectrophotometer to ensure the formation of nanoparticles. Gold and palladium nanoparticles showed strong SPR bands in the visible region, while others had broad and weak bands in the UV region (Huang and El-Sayed, 2010). The formation of Au-NPs and Au-Pd-NPs in the synthesized colloids was evaluated at a wavelength ranging from 500-550 nm. The appearance of this absorption peak showed the SPR characteristics of nanoparticles. The UV-Visible spectra of banana peel extract showed the presence of reductive compounds of flavonoid group, which were marked by a medium peak in the UV region. The UV-Visible characteristics of Au-NPs synthesized from banana peel extract were shown from the appearance of a medium peak at a wavelength of 550 nm. This was comparable to the low concentration of reductive compounds contained in banana peel extract, where lower absorption value, correlated with the number of gold particles. The formation of Au-Pd-NPs was indicated by the disappearance of the peak in the 550 nm region, showing a reduction in the characteristics of Au-NPs due to Pd skin formation.

Figure 4 shows the FTIR spectra of banana peel extract, Au-NPs, and Au-Pd-NPs. Banana peel used in this study comprised carbohydrate polymers (52.6%), which were mainly composed of lignin (9.13%), cellulose (34.61%), hemicellulose (6-8%), and pectin (1.92-3.25%). It also contained antioxidant compounds such as flavonoids (8.35%), tannins (29.01%), alkaloids (3.30%), and phenols (0.56%), serving as potential bioreductant agents in nanoparticle synthesis (Emaga et al., 2007). However, not all these compounds could be dissolved in water during the process of making banana peel extract. This was because only chemicals such as pectin, tannin, and phenol were soluble in water, playing an important role in the mechanism of nanoparticle synthesis.

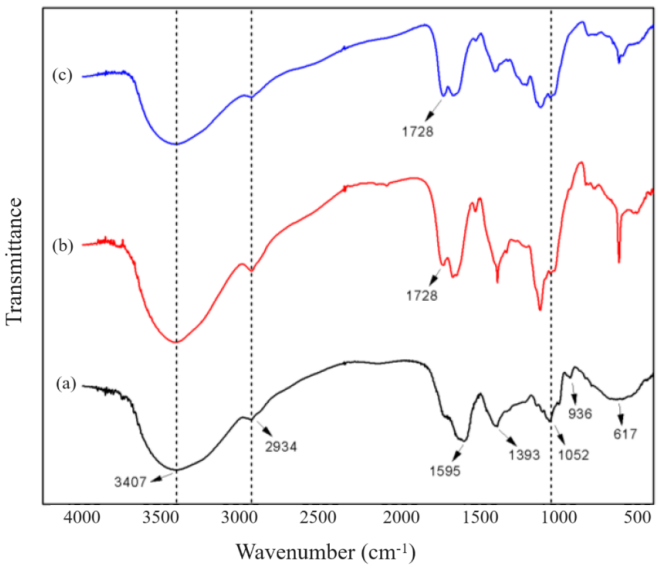

Figure 4. FTIR Spectra of (a) Banana Peel Extract, (b) Au-NPs, and (c) Au-Pd-NPs

The FTIR spectra showed that the absorption peak at wave number 3407 cm^{-1} was a special hydroxyl group (O−H) of carboxylic acid, related to the −OH of pectin structure or from water adsorption. The C−H functional group of alkanes was identified at wave number 2934 cm^{-1}, related to the −CH vibration in aliphatic hydrocarbons. The C−O group of carboxylic acid or ester was also identified at a wavelength of 1052 cm^{-1}. The absorption bands appearing at 1393 cm^{-1} and 1595 cm^{-1} refer to aromatic C=C, related to the vibration of the COOH group of pectin. The high intensity of the peaks at 1393 cm^{-1} and 1595 cm^{-1} compared to the peak at 1728 cm^{-1} showed that the carboxylate group was ionic. Subsequently, an absorption peak appeared at 936 cm^{-1} and 617 cm^{-1} due to the C−H vibration of carbohydrates. This showed that banana peel extract, namely pectin played a role in the nanoparticle synthesis process (Dmochowska et al., 2020).

The addition of $HAuCl_4$ and H_2PdCl_4 to banana peel extract caused a reduction, which was shown by the appearance of a peak in the wave number area of 1728 cm^{-1}. This was associated with the formation of the C=O group, showing the possible inclusion of banana peel extract. During this process, the chemicals in banana peel extract interacted with metals to allow the formation of nanoparticles (Bar et al., 2009). Accord-

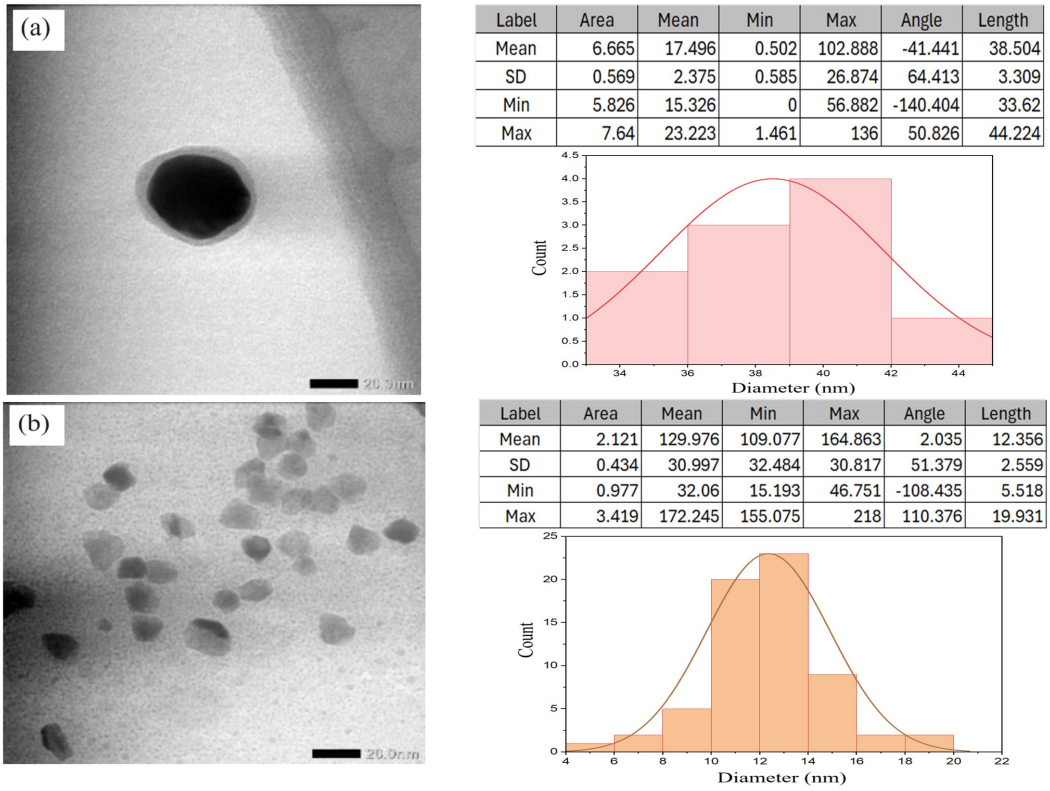

Figure 5. TEM Imaging, the Size and Distribution Particle of (a) Au-NPs and (b) Au-Pd-NPs

ing to Dmochowska et al. (2020), there were additional peaks in the spectrum of Au-NPs and Au-Pd-NPs. The appearance of an absorption peak around the wave number of 617 cm^{-1} was similar to the absorption band of banana peel extract adsorbed on the surface of materials.

TEM imaging results of Au-NPs and Au-Pd-NPs are shown in Figure 5. Based on the results, Au-NPs core had a spherical shape in the dark field with a diameter of 38.5 ± 3.3 nm (Figure 5a) and a Pd shell layer around the Au core in the bright field (Figure 5b) with a diameter of 12.4 ± 2.6 nm. The size and distribution of particles were processed using Image-J and Origin software. The results of the analysis obtained the distribution of particles of Au-NPs and Au-Pd-NPs shown in Figures 5a and 5b on the right. This showed a significant difference, where the particle size of Au-Pd-NPs was smaller than that of Au-NPs due to variations in synthesis methods and the properties of the materials (Zhan et al., 2011). The size of gold nanoparticles could be influenced by synthesis conditions, such as solution pH, temperature, and the presence of stabilizers (Sangwan and Seth, 2021). These factors caused variations in the nucleation and growth processes of nanoparticles, leading to larger particle sizes, and a significant impact of Pd shell around the gold core. Synthesis of core-shell nanoparticles often includes fine control of the shell thickness to achieve desired properties, such as catalytic activity or stability (Zhang et al., 2022). The Pd shell could limit the growth of gold core, leading to a smaller overall nanoparticle size compared to AuNPs. Additionally, steric hindrance provided by ligands attached to the nanoparticles could limit growth, particularly for those with a core-shell structure (Kapil et al., 2021). Ligands also showed the potential to create a physical barrier preventing further aggregation or growth, leading to smaller nanoparticles. The reaction mechanisms of Au-NPs and Au-Pd-NPs synthesis are shown in Figure 6.

3.2 Electrochemical Response of Au-NPs and Au-Pd-NPs

Electrochemical performance of Au-Pd-NPs working electrode was evaluated using CV in the ferricyanide system. The potential range used during testing was -0.65 to 0.5 V and the scan rate varied from 0.01 to 0.03 V/s. The reduction-oxidation reaction that occurred in the $[Fe(CN)_6]/K_4[Fe(CN)_6]$ solution system was the reaction:

$$[Fe(CN)_6]^{4-} \rightarrow [Fe(CN)_6]^{3-} + e^- \text{ (oxidation)}$$
$$[Fe(CN)_6]^{3-} + e^- \rightarrow [Fe(CN)_6]^{4-} \text{ (reduction)}$$

Figure 7 shows the voltammogram cyclic of Au-NPs and Au-Pd-NPs electrodes in ferricyanide solutions. Oxidation peaks were observed at potential between 0.15 to 0.25 V and reduction peaks at -0.6 to -0.35 V. This showed the occurrence

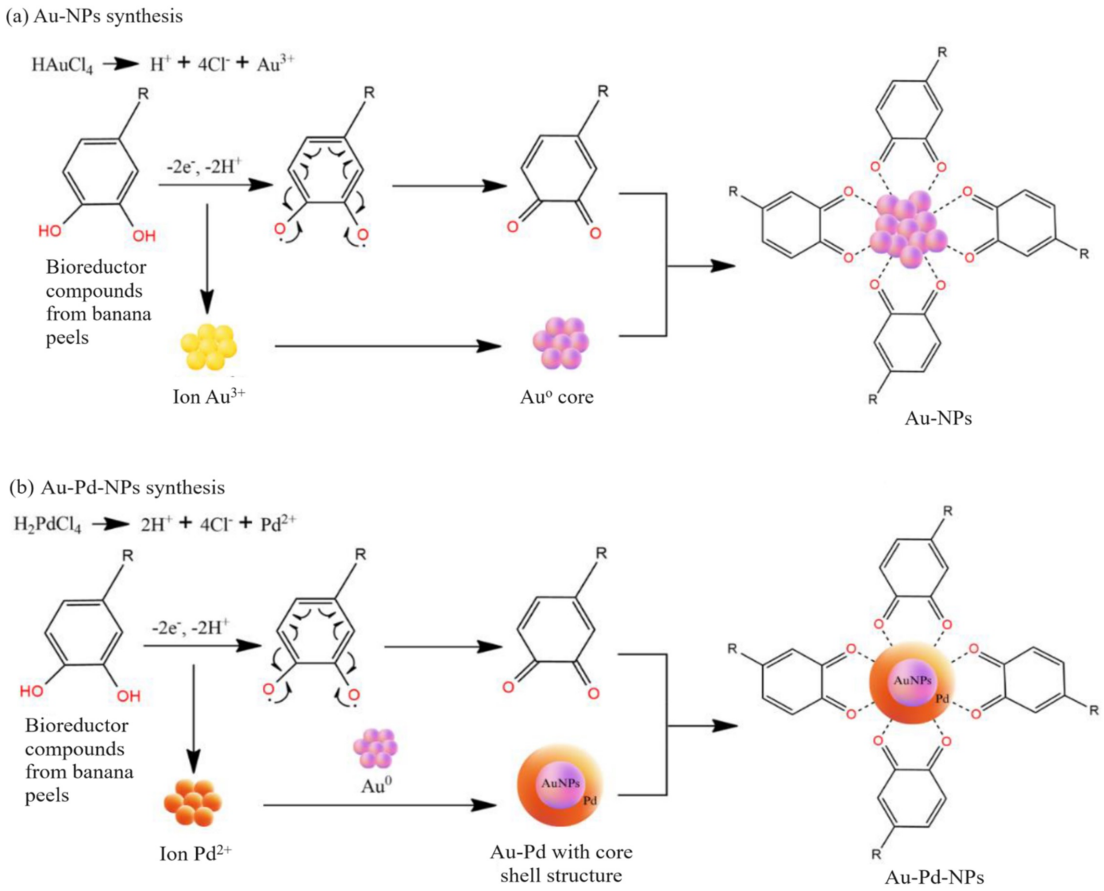

Figure 6. Reaction Mechanism in the Synthesis of Au-NPs (a) and Au-Pd-NPs (b)

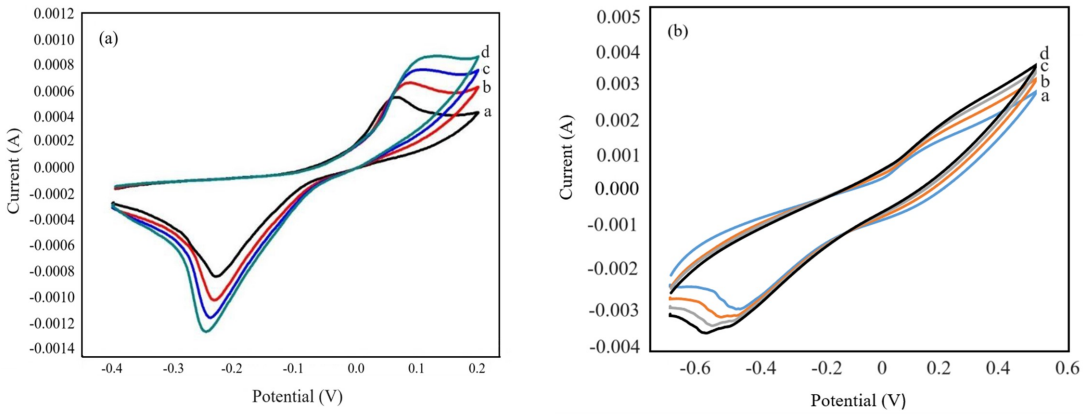

Figure 7. Voltammogram of Electrochemical Response of Au-NPs (a) and Au-Pd-NPs (b) Electrodes in $K_3[Fe(CN)_6]/K_4[Fe(CN)_6]$ Solution with Scan Rate of 0.010 (a) 0.015 (b) 0.020 (c) and 0.025 V/sec, with 1M KCl Electrolyte

of a reversible redox reaction in ferricyanide solutions in 1 M KCl. The redox couple $[Fe(CN)_6]^{3-}/[Fe(CN)_6]^{4-}$ is a fast electrochemical reaction with a 1 electron transfer process. The relationship between the scan rate and the peak oxidation current showed that electron transfer from the ferricyanide solutions system to the nanoparticles surface was controlled by diffusion. The $[Fe(CN)_6]^{3-}/[Fe(CN)_6]^{4-}$ ions interacted with the nanoparticles' surface and formed a chemisorption layer on the electrode surface, providing a signal to form a voltammogram. Based on electrochemical response, the Au-Pd-NPs electrode showed potential for use as an electrode for hydroquinone analysis.

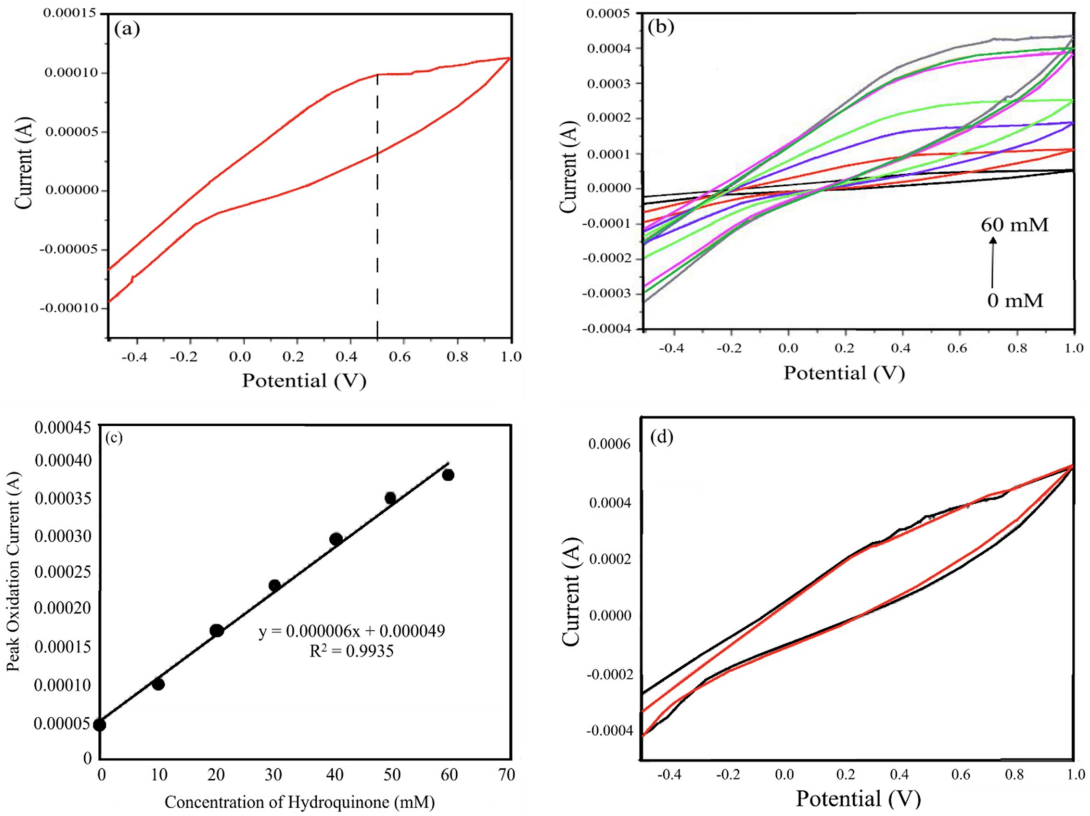

Figure 8. Voltammogram of Au-Pd-NPs Electrode Against 10 mM Hydroquinone Solution (a) 0-60 mM Hydroquinone (b) Calibration Curve (c) and Cosmetics Cream Sample (d), with Phosphate-Buffered

3.3 Application of Au-Pd-NPs for Hydroquinone Analysis

Figure 8a shows the response of Au-Pd-NPs to hydroquinone with PBS electrolyte at pH 7.0, ensuring the appearance of hydroquinone oxidation peak. Meanwhile, Figure 8b shows the voltammogram with variations in hydroquinone concentration. The appearance of oxidation peak at a potential of 0.5 V (Figure 8a) shows that the bimetallic metal nanoparticle electrode (Au-Pd-NPs) has good catalytic and conductivity properties suitable for use as electrocatalyst. At this potential, hydroquinone is oxidized on the surface of Au-Pd-NPs working electrode. The presence of Au and Pd metals facilitates the electron transfer process to become faster, leading to the production of higher oxidation peak during testing. Figure 8c shows a linear regression equation with an R^2 value of 0.9935, which indicates that hydroquinone concentration is directly proportional to the oxidation current peak.

The results of cosmetics cream sample tests carried out in the first and second repetitions were shown in Figure 8d, which obtained hydroquinone levels of 1.34% and 1.31%, respectively. These values were within the permitted limit according to Cosmetic Safety Regulation of the EU, which allowed a maximum concentration of 2% (Lin et al., 2005). This method has a LOD and LOQ of 0.07% and 0.11%, respectively. This method also has very good accuracy with a Relative Percent Difference (%RPD) of 2.26%. This %RPD is still acceptable because it is lower than 0.5% Horwitz's relative standard deviation (0.5% RSD Horwitz) of 7.67%. However, the limitation observed was the wide oxidation and reduction peak of the composite. Electrochemical response of the working electrode was also influenced by electrolytes, the charge transfer reaction at the electrode interface, as well as size and shape of electrode (González et al., 2022).

4. CONCLUSIONS

In conclusion, this study showed that banana peel extract could be used as bioreductor agent for synthesis of Au-NPs and Au-Pd-NPs, as confirmed by the characterization methods, including UV-Visible Spectrophotometer, FTIR, and TEM. The addition of Pd metal to Au-NPs had a positive effect on the particle size and enhanced the performance of nanoparticles. Based on electrochemical response, Au-Pd-NPs electrode was better than Au-NPs, making it an alternative electrode for detecting hydroquinone in cosmetics. For further optimization of Au-Pd-NPs performance, the development of composite electrode with small surface area was recommended to obtain a sharp peak.

5. ACKNOWLEDGMENT

The authors are grateful to the Ministry of Education, Culture, Research, and Technology of Indonesia for the financial support provided through study grants No. 107/E5/PG.02.00.PL/2024, No. 0609.1/LL5-INT/AL.04/2024, and No. 054/DirD PPM/70/DPPM/PTM-KEMDIKBUDRISTEK/VI/2024.

REFERENCES

Adebajo, S. (2002). An Epidemiological Survey of the Use of Cosmetic Skin Lightening Cosmetics Among Traders in Lagos, Nigeria. *Mercury*, **5**(7); 43–48

Aziz, M., T. Selvaraju, and H. Yang (2007). Selective Determination of Catechol in the Presence of Hydroquinone at Bare Indium Tin Oxide Electrodes via Peak-Potential Separation and Redox Cycling by Hydrazine. *Electroanalysis*, **19**(14); 1543–1546

Bar, H., D. Bhui, G. Sahoo, P. Sarkar, S. Pyne, and A. Misra (2009). Green Synthesis of Silver Nanoparticles Using Seed Extract of *Jatropha Curcas*. *Colloids and Surfaces A: Physicochemical and Engineering Aspects*, **348**(1–3); 212–216

Bhardwaj, J., S. Devarakonda, S. Kumar, and J. Jang (2017). Development of a Paper-Based Electrochemical Immunosensor Using an Antibody-Single Walled Carbon Nanotubes Bio-Conjugate Modified Electrode for Label-Free Detection of Foodborne Pathogens. *Sensors and Actuators B: Chemical*, **253**; 115–123

Bindhu, M. and M. Umadevi (2013). Synthesis of Monodispersed Silver Nanoparticles Using *Hibiscus cannabinus* Leaf Extract and Its Antimicrobial Activity. *Spectrochimica Acta Part A: Molecular and Biomolecular Spectroscopy*, **101**; 184–190

Chafidz, A., A. Afandi, B. Rosa, J. Suhartono, P. Hidayat, and H. Junaedi (2020). Production of Silver Nanoparticles via Green Method Using Banana Raja Peel Extract as a Reducing Agent. *Communications in Science and Technology*, **5**(2); 112–118

Chakti, A., E. Simaremare, and R. Pratiwi (2019). Analisis Merkuri dan Hidrokuinon pada Krim Pemutih yang Beredar di Jayapura. *Jurnal Sains dan Teknologi*, **8**(1); 1–11

Desiderio, C., L. Ossicini, and S. Fanali (2000). Analysis of Hydroquinone and Some of Its Ethers by Using Capillary Electrochromatography. *Journal of Chromatography A*, **887**(1-2); 489–496

Dmochowska, A., J. Czajkowska, R. Jędrzejewski, W. Stawiński, P. Migdał, and M. Fiedot-Toboła (2020). Pectin Based Banana Peel Extract as a Stabilizing Agent in Zinc Oxide Nanoparticles Synthesis. *International Journal of Biological Macromolecules*, **165**; 1581–1592

Du, X., X. Zheng, Z. Zhang, X. Wu, L. Sun, J. Zhou, and M. Liu (2019). A Label-Free Electrochemical Immunosensor for Detection of the Tumor Marker CA242 Based on Reduced Graphene Oxide-Gold-Palladium Nanocomposite. *Nanomaterials*, **9**(9); 1335

Elferjani, H., N. Ahmida, and A. Ahmida (2017). Determination of Hydroquinone in Some Pharmaceutical and Cosmetic Preparations by Spectrophotometric Method. *International Journal of Scientific Research*, **6**; 2219–2224

Emaga, T., R. Andrianaivo, B. Wathelet, J. Tchango, and M. Paquot (2007). Effects of the Stage of Maturation and Varieties on the Chemical Composition of Banana and Plantain Peels. *Food Chemistry*, **103**; 590–600

González, J., E. Laborda, and A. Molina (2022). Voltammetric Kinetic Studies of Electrode Reactions: Guidelines for Detailed Understanding of Their Fundamentals. *Journal of Chemical Education*, **100**(2); 697–706

Huang, X. and M. El-Sayed (2010). Gold Nanoparticles: Optical Properties and Implementations in Cancer Diagnosis and Photothermal Therapy. *Journal of Advanced Research*, **1**(1); 13–28

Kapil, N., F. Cardinale, T. Weissenberger, P. Trogadas, T. Nijhuis, M. Nigra, and M. Coppens (2021). Gold Nanoparticles with Tailored Size Through Ligand Modification for Catalytic Applications. *Chemical Communications*, **57**(82); 10775–10778

Khan, I., K. Saeed, and I. Khan (2019). Nanoparticles: Properties, Applications and Toxicities. *Arabian Journal of Chemistry*, **12**(7); 908–931

Khoshroo, A., M. Mazloum-Ardakani, and M. Forat-Yazdi (2018). Enhanced Performance of Label-Free Electrochemical Immunosensor for Carbohydrate Antigen 15-3 Based on Catalytic Activity of Cobalt Sulfide/Graphene Nanocomposite. *Sensors and Actuators B: Chemical*, **255**; 580–587

Kumar, N. and R. Goyal (2017). Gold-Palladium Nanoparticles Aided Electrochemically Reduced Graphene Oxide Sensor for the Simultaneous Estimation of Lomefloxacin and Amoxicillin. *Sensors and Actuators B: Chemical*, **243**; 658–668

Lei, Y., G. Zhao, M. Liu, X. Xiao, Y. Tang, and D. Li (2007). Simple and Feasible Simultaneous Determination of Three Phenolic Pollutants on Boron-Doped Diamond Film Electrode. *Electroanalysis*, **19**(18); 1933–1938

Li, Y., J. He, J. Chen, Y. Niu, Y. Zhao, Y. Zhang, and C. Yu (2018). A Dual-Type Responsive Electrochemical Immunosensor for Quantitative Detection of PCSK9 Based on n-C60-PdPt/N-GNRs and Pt-Poly (Methylene Blue) Nanocomposites. *Biosensors and Bioelectronics*, **101**; 7–13

Lin, C., J. Sheu, H. Wu, and Y. Huang (2005). Determination of Hydroquinone in Cosmetic Emulsion Using Microdialysis Sampling Coupled with High-Performance Liquid Chromatography. *Journal of Pharmaceutical and Biomedical Analysis*, **38**(3); 414–419

Liu, C., J. Dong, G. Waterhouse, Z. Cheng, and S. Ai (2018). Electrochemical Immunosensor with Nanocellulose-Au Composite Assisted Multiple Signal Amplification for Detection of Avian Leukosis Virus Subgroup. *J. Biosensors and Bioelectronics*, **101**; 110–115

Liu, S., Y. Shen, C. Chiu, S. Rej, P. Lin, Y. Tsao, and M. Huang (2015). Direct Synthesis of Palladium Nanocrystals in Aqueous Solution with Systematic Shape Evolution. *Langmuir*,

31(23); 6538–6545
Melisa, C. and W. Jay (2009). FDA Proposes Hydroquinone Ban. *J Cul Afr Wmn Stds*, **14**; 5–16
Mersal, G. (2009). Electrochemical Sensor for Voltammetric Determination of Catechol Based on Screen Printed Graphite Electrode. *International Journal of Electrochemical Science*, **4**(8); 1167–1177
Nurhan, A., T. Mu, N. Rizki, E. Zuhrufi, G. Putri, and M. Firdaus (2017). Pengetahuan Ibu-Ibu Mengenai Kosmetik Yang Aman Dan Bebas Dari Kandungan Bahan Kimia Berbahaya. *Jurnal Farmasi Komunitas*, **4**(1); 15–19
Pereira, M., R. de Souza Paiva, T. Vasconcelos, A. Oliveira, M. Salles, H. Toma, and D. Grasseschi (2020). Photoinduced Electron Transfer Dynamics of AuNPs and Au@ PdNPs Supported on Graphene Oxide Probed by Dark-Field Hyperspectral Microscopy. *Dalton Transactions*, **49**(45); 16296–16304
Pistonesi, M., M. Di Nezio, M. Centurión, M. Palomeque, A. Lista, and B. Band (2006). Determination of Phenol, Resorcinol and Hydroquinone in Air Samples by Synchronous Fluorescence Using Partial Least-Squares (PLS). *Talanta*, **69**(5); 1265–1268
Sangwan, S. and R. Seth (2021). Synthesis, Characterization and Stability of Gold Nanoparticles (AuNPs) in Different Buffer Systems. *Journal of Cluster Science*; 1–16
Shore, A., Z. Mazzochette, and A. Mugweru (2016). Mixed Valence Mn, La, Sr-Oxide Based Magnetic Nanoparticles Coated with Silica Nanoparticles for Use in an Electrochemical Immunosensor for IgG. *Microchimica Acta*, **183**; 475–483
Siddique, S., Z. Parveen, Z. Ali, and M. Zaheer (2012). Qualitative and Quantitative Estimation of Hydroquinone in Skin Whitening Cosmetics. *Journal of Cosmetics, Dermatological Sciences and Applications*, **2**(3); 224
Sotomayor, M., A. Tanaka, and L. Kubota (2022). Development of an Enzymeless Biosensor for the Determination of Phenolic Compounds. *Analytica Chimica Acta*, **455**(2); 215–223
Thongnopkun, P., M. Jamkratoke, and Y. Jitkam (2018). Green Synthesis and Characterization of Silver Nanoparticle Using Natural Reducing Sugar from Cultivated Banana Peel. *Journal of Physics: Conference Series*, **1144**; 012159
Tsai, Y. and C. Chiu (2007). Amperometric Biosensors Based on Multiwalled Carbon Nanotube-Nafion-Tyrosinase Nanobiocomposites for the Determination of Phenolic Compounds. *Sensors and Actuators B: Chemical*, **125**(1); 10–16
Wang, L., Y. Zhang, A. Wu, and G. Wei (2017). Designed Graphene-Peptide Nanocomposites for Biosensor Applications: A Review. *Analytica Chimica Acta*, **985**; 24–40
Westerhof, W. and T. Kooyers (2005). Hydroquinone and Its Analogues in Dermatology-A Potential Health Risk. *Journal of Cosmetic Dermatology*, **4**(2); 55–59
Zhan, G., J. Huang, M. Du, I. Abdul-Rauf, Y. Ma, and Q. Li (2011). Green Synthesis of Au-Pd Bimetallic Nanoparticles: Single-Step Bioreduction Method with Plant Extract. *Materials Letters*, **65**(19-20); 2989–2991
Zhang, Y., Y. Huang, H. Chen, X. Luo, J. Zhang, H. Wang, and S. Wang (2022). Design of a Nanocomposite with Gold Nanoparticles as the Core and Casein-Templated Gold Nanoclusters as the Shell with Ultra-Low Protein Corona for Enhanced Photodynamic Therapy. *Materials Advances*, **3**(23); 8438–8448
Zhao, D., X. Zhang, L. Feng, L. Jia, and S. Wang (2009). Simultaneous Determination of Hydroquinone and Catechol at PASA/MWNTs Composite Film Modified Glassy Carbon Electrode. *Colloids and Surfaces B: Biointerfaces*, **74**(1); 317–321

